Journal of
APPLIED
BIOMEDICINE

J Appl Biomed. **11**: 143–151, 2013
DOI 10.2478/v10136-012-0017-8
ISSN 1214-0287

ORIGINAL ARTICLE

Computational modeling in the prediction of Dynamic Hip Screw failure in proximal femoral fractures

Maroš Hrubina[1, 2], **Zdeněk Horák**[3], **Radek Bartoška**[4], **Leoš Navrátil**[2], **Jozef Rosina**[2]

[1]Department of Orthopaedics, Hospital Pelhřimov, Czech Republic
[2]Czech Technical University in Prague, Faculty of Biomedical Engineering, Department of Medicine and Humanities, Kladno, Czech Republic
[3]Czech Technical University in Prague, Faculty of Mechanical Engineering, Laboratory of Biomechanics, Prague, Czech Republic
[4]Department of Orthopaedics and Traumatology, Third Medical Faculty of Charles University and University Hospital Královské Vinohrady, Prague, Czech Republic

Received 10th February 2012.
Revised 6th April 2012.
Published online 10th April 2012.

Summary
The aim of the study was to determine the relationship between implant-associated complications and Dynamic Hip Screw (DHS) placement in the femoral neck, based on a Finite Element (FE) Analysis. Very diverse implant failures and subsequent complications can be encountered after introduction of the DHS. We evaluated 308 dynamic hip screw osteosyntheses for pertrochanteric fractures in 297 patients. The ABAQUS 6.9 program was used for development of the FE model, and the analyses were performed in 5 modelled situations corresponding to five different screw locations. Complications occurred in 10% of patients and re-operation was necessary in 3.9%. The highest risk of implant failure was associated with the screw situation in the upper third of the femoral neck. Placing a dynamic hip screw in the middle third of the neck significantly reduced stresses in the plate and screw. The screw position in the upper third of the neck significantly increased these stresses. The finite element analysis confirmed our clinical experience that the optimum position of the dynamic hip screw is in the middle third of the femoral neck.

Key words: dynamic hip screw; proximal femoral fracture; finite element method

INTRODUCTION

Proximal femoral fractures are a serious medical and economic problem, the importance of which increases in an ageing population. In the Czech Republic, in persons over 50 years of age they occur in 195.2/100,000 men and 259.4/100,000 woman annually (Vaculik et al. 2007); the highest incidence of 1.32% was noted in patients over 85 years of age (Füchtmeier et al. 2011). While the available literature offers a sufficient source of classification and treatment options (Bartonicek et al. 2002, Bonnaire et al. 2011), less attention has been paid to implant failures and their causes (Baumgaertner et al. 1995). The Dynamic Hip Screw (DHS) is an implant making possible the controlled impaction and stable contact of femoral fragments during fracture healing because the hip screw slides in the hip plate (Fig. 1). It is suitable for the treatment of stable pertro-

✉ Maroš Hrubina, Department of Orthopaedics, Hospital Pelhřimov, Slovanského bratrství 710, 393 01 Pelhřimov, Czech Republic
💻 mhrubina@gmail.com
☎ +420 728 312 008

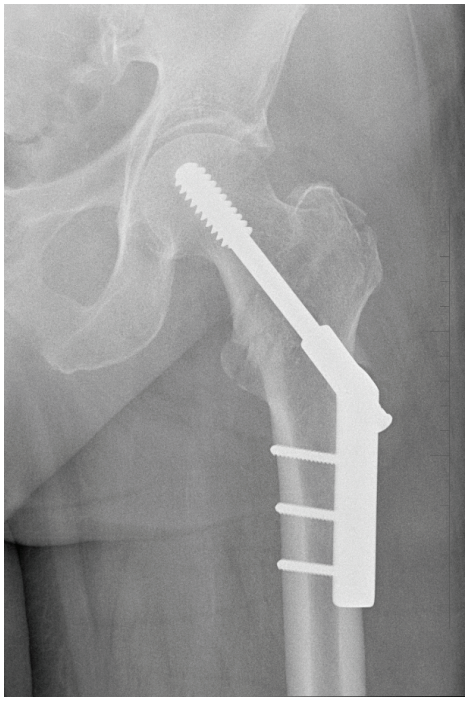

Fig. 1. **A woman aged 81 years with pertrochanteric femoral fracture treated with the Dynamic Hip Screw.**

chanteric fractures. We have used this method since 1997 and at the end of 2010 we had made more than 500 such implants. The specific complication rate in patients with stable pertrochateric fractures is 10% (Hrubina et al. 2010). Our interest was particularly focused on the cause of failure in cases which our clinical experience indicated could lead to potentially dangerous situations Therefore the aim of the study was to evaluate specific implant-associated complications after the treatment of stable pertrochanteric fractures by dynamic hip screw, resulting from the femoral neck screw positioning. We compared these clinical results with a geometric model of the proximal femur and numerical simulations.

MATERIAL AND METHODS

The work was approved by the Ethical Committee of the Pelhřimov Hospital, in which it was performed, and informed consent was obtained from all the subjects treated. The group studied consisted of 297 patients over 50 years of age, in which 308 DHS osteosyntheses were performed. Eleven patients were operated on both sides. In all the cases in the period 1997–2008 we treated stable pertrochanteric fractures by using 135°, 1″collar, 3-holes hip plate with DHS 95 mm and 3 cortical screws (Medin, a. s., Nové Město na Moravě, Czech Republic). The follow-up period was two years.

We provided a standard diagnosis based on the assessment of anteroposterior X-ray of the injured hip joint. The group included patients with stable pertrochanteric fractures only (31-A1.1, 31-A1.2 according to AO classification). The operation was performed in a standard way under spinal anesthesia. The post-operative care of patients was carried out in an intensive care unit for one or two days after the surgery and after that in a standard department. Mobilization and walking with crutches was conducted from the third to fourth days after the surgery. Walking with crutches with no weight bearing was recommended at least till the first control X-ray examination 6 weeks after the operation. Full weight bearing was recommended in cases with good clinical and radiological outcomes 12 weeks after the surgery. Further clinical and X-ray examinations were performed at intervals of 6, 12 and 24 months. When evaluating radiographs, a blinded examiner observed the signs of fracture healing, fragmental compression (gradual prominence of the hip screw laterally), changes in the screw position or protrusion from the femoral head ("cut-out" phenomenon), osteosynthetic material breaking or nonunion (Fig. 2). An implant failure was defined by the necessity for reoperation. X-ray findings were divided into 5 subgroups according to the femoral neck screw – DHS position.

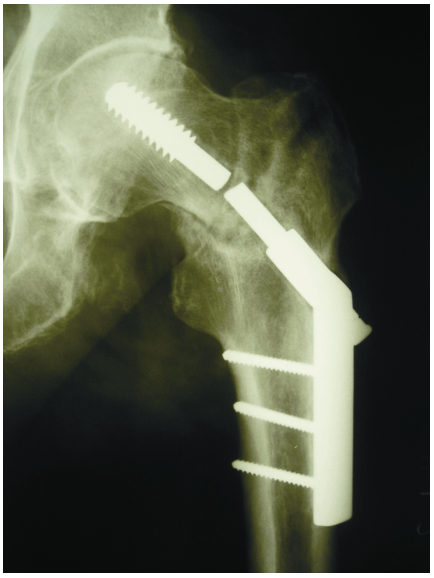

Fig. 2. **A patient aged 59 years 11 months after the DHS osteosynthesis for proximal femoral fracture.** The screw was broken due to insufficient fragment reduction and nonunion.

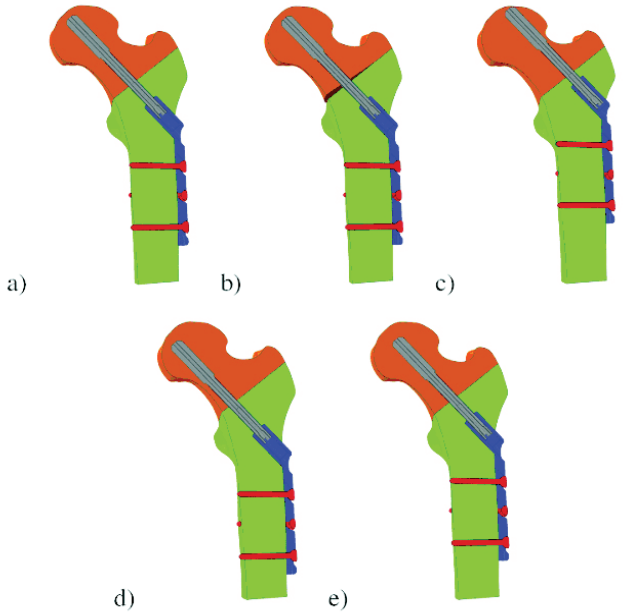

Fig. 3. **Five model positions of the DHS in the femoral neck.** The optimum placement in the middle third of the neck Fig. 3a, corresponds with model 0 and position 2. Fig. 3b, with opened fracture line medially corresponds with model I and position 4. Fig. 3c, with location of the screw in the upper third of the neck associated with the highest risk of complications corresponds with model IIa and position 1. Fig. 3d, with screw location in the lower third of the neck corresponds with model IIb and position 3. Fig. 3e, with no subchondral screw fixation corresponds with model III and position 5.

Subsequently, according to the 5 observed variants of the DHS location in the femoral neck in our group of patients, the computational models for each of the five subgroups were developed. For our own evaluation of the numerical model in relation to the clinical group of patients and failures, we simulated the following 5 situations:

Position 1 (model IIa) – DHS location along the axis of the femoral neck, in upper third of the neck with subchondral fixation (Figs 3c, 4c).

Position 2 (model 0) – DHS location in the middle third of the femoral neck with subchondral fixation (Figs 3a, 4a) – the ideal situation.

Position 3 (model IIb) – DHS location in the lower third of the femoral neck with subchondral fixation (Figs 3d, 4d).

Position 4 (model I) – DHS location in the middle third of the femoral neck with subchondral fixation and opening the fracture line distally and medially (Figs 3b, 4b).

Position 5 (model III) – DHS location in the middle third of the femoral neck with the screw fixation at the femoral head centre (Figs 3e, 4e).

Standard parameters (based on our clinical observation) for the model were first determined – starting position:

a, proximal femur with collum-diaphysis angle 135° of the femoral neck with 15° of anteversion;
b, stable pertrochanteric fracture – the fracture line is extended just above the lesser trochanter, ventrally in the area of *linea intertrochanterica*, where the reference points were selected one third the distance between *tuberculum trochantericum* and *tuberculum innominatum*, dorsally in the area of *crista intertrochanterica* (Fig. 3a);
c, the possibility of the fracture line opening medially in the Adams arch by 4 mm (based on our clinical observation of fractures, where the opening was about 3–5 mm in 19 cases) (Fig. 3b);
d, the femoral neck screw placement has always been provided centrally in the femoral neck and head in the axial projection.

Only one realistic femur model was employed to perform the whole parametric Finite Element Analysis, which was designed to determine general trends, not the responses of individual patients to the external load during the use of a particular fixation system. The geometric model of the proximal femur was developed from a series of CT-scans of healthy individuals. Only one set of CT images from a healthy man aged 55 years was used. A total of 473 femoral bone transverse sections were provided.

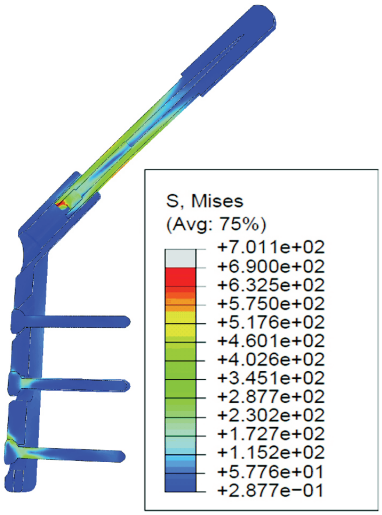

a

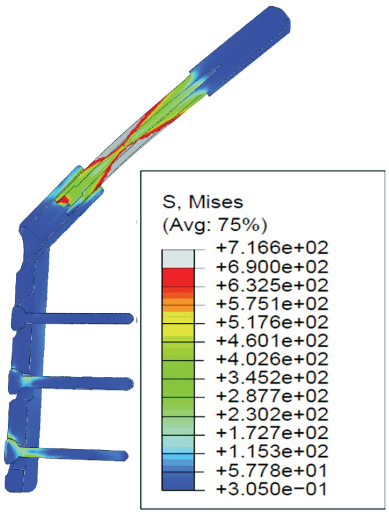

b

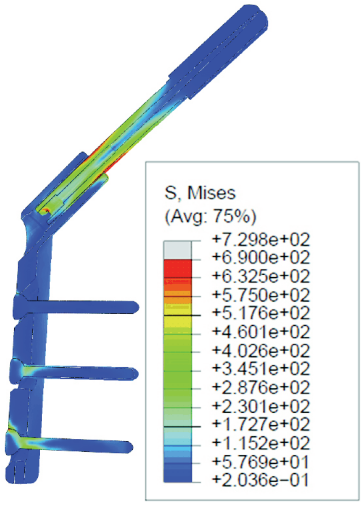

c

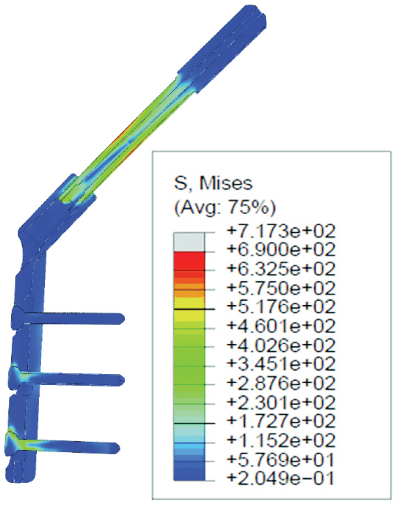

d

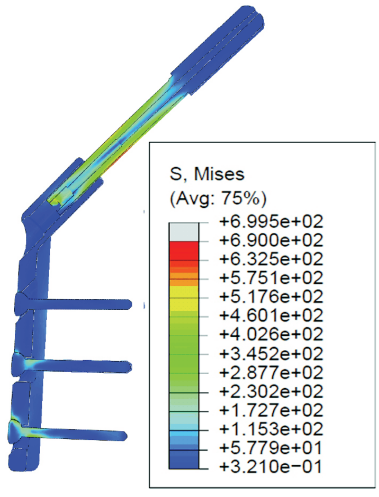

e

Fig. 4. **The equivalent stress distribution** (von Mises stress) σ_{HMH} [MPa] in the neck screw and hip plate in 5 model situations. The highest risk of complications is shown in Fig. 4c due to the stress distribution in the whole model. Fig. 4a corresponds with Fig. 3a, and model 0. Fig. 4b, corresponds with Fig. 3b and model I with V-shaped cut between the bone fragments. In this position there is the highest value of the reduced stress in the neck screw.The implant failure rate is low due to the possibility of the fragment compression in the course of fracture healing. Fig. 4c, corresponds with Fig. 3c, and model IIa. Fig. 4d corresponds with Fig. 3d, and model IIb. Fig. 4e corresponds with Fig. 3e and model III.

The images were taken at a resolution of 512 × 512 pixels, the pixel size was 0.412 mm and the distances between slices were 0.5 mm. CT images in the DICOM format were imported into the software Mimics 12 (Materialise, Belgium), to perform the three-dimensional recovery of the femoral fragments. The geometric model was obtained by using a surface triangle mesh, which was imported into the ABAQUS 6.9 program in the format *.inp. In this program the volume FEM (Finite Element Method) mesh was subsequently automatically generated from the surface structure. The screw thread was not included in the model. The DHS and cortical screws threads were replaced by a smooth surface, the size of which corresponded to the mean diameter of the thread. Individual parts of the broken femur, DHS and fixation cortical screws were created by volume linear tetrahedron C3D4 elements. The FEM was used to evaluate the stress and strain response of the bone model to the load. As a limit state, a failure occurs if fixation elements or failure of their attachment to the bone are exposed to a load which causes stress exceeding the yield stress (σ_k) or strength (R_m) in any part of the modeled system DHS – hip plate – cortical screws – bone.

The resulting use of the numerical models is shown in Fig. 3. The DHS model was provided by Medin in the format * .SAT, which was imported into ABAQUS 6.9 (Simulia, France). The stainless steel used to produce the DHS was modelled as a homogeneous isotropic and elastio-plastic material in all the numerical FE analyses with elastic modulus E=210 GPa, Poisson's ratio μ= 0.3, strength R_m=860 MPa and yield stress σ_k=690 MPa. In all the analyses performed, the bone tissue was modelled as a homogeneous, isotropic and elastio-plastic material (Baca et al. 2007). Material properties were determined for each element depending on the density of bone tissue ρ [g/cm^3]. This density was determined depending on the degree of the gray shade in the proximal femoral CT scans according to the equation (1)

$$\rho = 1.54 \cdot \rho CT + 0.0784 \qquad (1)$$

where ρ [g/cm^3] is the density of the calibration sample. The moduli of elasticity E [MPa] were determined for both compact (superscript "c") and spongious (superscript "s") types of the bone tissue by using the equations (2–3).

$$E^c = 2065\,\rho^{3.09} \quad , \quad \mu^c = 0.3$$
$$E^s = 1904\,\rho^{1.64} \quad , \quad \mu^s = 0.3 \qquad (2)$$

In the same way, the yield stress σ_k [MPa] was set as a function dependent on the value of bone density by

$$\sigma_k^c = 57.75\,\rho^{1.73} \quad \text{for} \quad \rho \geq 0.945$$
$$\sigma_k^s = 76.5\,\rho^{6.7} \quad \text{for} \quad \rho < 0.945 \qquad (3)$$

In the FE analyses, the bone tissue was also modelled as a material producing degradation of its mechanical properties on exceeding the limit stress (Baca et al. 2008).

Particular situations were analysed by using numerical FE simulations taking into account biomechanical conditions expressed by compression of the fragments during the fracture healing. The aim of the analysis performed was to determine the bone response to load in the proximal part of the femur depending on the implant situation. The loading was realized by applying single external forces acting from *musculus iliopsoas*, *musculi glutei* and the reaction involved in the hip joint. For the application of external forces in the FE model a distributed coupling interaction was used, through which the individual forces applied at the reference node were evenly distributed within the bone tissue at the muscle attachment and femoral head contact with the acetabulum. During the analyses performed the model was exposed to individual forces F_{glut} = 642.3 N, F_{iliop} = 376.4 N a F_{reac} = 1000 N loading the hip joint of a walking individual weighing 80 kg.

Among femoral fragments a normal contact of type "HARD" with a coefficient of friction f=0.3 was modelled. This contact simulated a real situation, in which there is no mutual penetration of individual parts, but their mutual compression is possible. The contact relations between the DHS and the bone (f=0.3), between the DHS and the hip plate (f=0.15) and between the hip plate and the bone (f=0.3) were modelled in the same way. The bone interaction with cortical screws, the hip plate interaction with cortical screws and DHS interaction with bone was due to the calculation speed and stability modelled by using a TIE contact in each case. This specific type of contact represents a fixed combination of two parts, where the nodes of both contact parts have a firm mutual coupling. This coupling transfers the same value for the size of the displacement from the master contact surface to the slave.

Our Finite Element Model and the Finite Element Method of the analysis were verified in our previous works: Baca et al. (2007, 2008), where we demonstrated a very good agreement of the computational model with outcomes of clinical practice and anatomical relationships between the bone tissue design and structure. The method was also compared with conclusions by Viceconti et al. (2005).

RESULTS

The age of patients in the study cohort ranged from 50 to 102 years with an average age of 84 years. 263 (88.5%) patients were over 70 years of age. Lateral involvement was balanced (153 times on the right side, 155 times on the left side). The DHS was performed bilaterally in 11 patients at intervals of 4–42 months after the previous osteosynthesis. Among 308 osteosyntheses performed and analysed, we encountered a total of 31 specific implant-associated complications (10%). Twelve patients with 12 DHS (3.9%) were re-operated on because of the implant failure. The incidence of complications in the each of the 5 observed positions is shown in Table 1.

Table 1. **The number of DHS divided according to the position of the neck screw into 5 groups.**

	DHS	Complications		Reoperations	
Position 1 (model IIa)	3	3	(100%)	3	(100%)
Position 2 (model 0)	146	13	(9%)	5	(3%)
Position 3 (model IIb)	130	12	(9%)	3	(2%)
Position 4 (model I)	19	1	(5%)	0	(0%)
Position 5 (model III)	10	2	(20%)	1	(10%)
Total	308	31	(10%)	12	(3.9%)

There were only 3 osteosyntheses in position 1, but the "cut-out" with a need for re-operation was found in all of them.

Position 2 – there were 13 specific complications (1× non-union with DHS breakage, 2× cortical screws breakage, 2× "cut-out", 8× changed screw position). We re-operated 5 patients with osteosynthetic material breakage and "cut-out". Eight patients with changed screw position during the fracture healing (a screw proximalisation from the middle third to the upper third of the neck) were without need for re-operation.

Position 3 – there were 12 specific complications (1× non-union with DHS breakage, 2× "cut-out", 9× changed screw position). We re-operated 3 patients with metal breakage and "cut-out".

Position 4 – there was only one patient with a screw proximalisation without need for re-operation.

Position 5 – there were 2 specific complications (1× "cut-out", 1× changed screw position) with the need for re-operation of "cut-out".

From Table 1 it is obvious that the most serious problem was the DHS location in position 1, which required re-operation in all the cases, and in position 5, where we had to re-operate in 50% of cases.

All the numerical analyses performed were modelled as contact, non-linear and static tasks, during which we tried to detect the response of the whole system to the loading applied. While solving these tasks, the numerical FE analyses took into consideration the local mechanical properties of the bone tissue. The FE analysis results obtained are summarized in Table 2 and in Fig. 4. From the results of FE simulations listed in Table 2 it is clear that there was a significant stress in the whole model of the femur and DHS with the hip plate during the load application. In all the models, the bone tissue of the femur (distal fragment "bottom") is exposed to the greatest load in the area of the third – lowermost cortical screw, which fixates the hip plate to the femur. In this part of the bone the maximum reduced stress σ_{HMH} value fluctuates in a range of 164.2 MPa (model III) to 192.9 MPa (model IIa). In this section of the model, we also found clear damage to the bone tissue at the level of the fracture plane and the hole of the femoral neck screw. In all the models except model I, the femoral bone (proximal fragment –"Top") is most loaded at the lower edge of the femoral neck along the fracture line. At this point there is a compression of proximal and distal fragments. The maximum values of the stress σ_{HMH} are in a range from 106.7 MPa (model IIa) to 165.0 MPa (model III). In contrast, model I shows a maximum load of the bone tissue at the hole in which

Table 2. **The resultant values of the reduced stress σ_{HMH} [MPa] in particular parts of FE model proximal femur and DHS.**

	Proximal bone fragment "Top" σ_{HMH} [MPa]	Distal bone fragment "Bottom" σ_{HMH} [MPa]	Hip plate σ_{HMH} [MPa]	DHS σ_{HMH} [MPa]	Cortical screws σ_{HMH} [MPa]
Model 0	170.63	192.94	436.53	435.31	693.10
Model I	83.12	168.51	703.80	716.64	695.52
Model IIa	106.70	192.92	729.81	713.83	706.63
Model IIb	123.91	192.90	717.33	698.12	698.21
Model III	165.00	164.22	699.52	691.62	698.44

the DHS is located (near the fracture plane). In evaluating the bone tissue response to external loading in various DHS locations, the type of stress distribution was found to be of importance. Even the distribution of the tension in the whole volume of the femoral head and neck is important for successful DHS implantation. An optimum situation is shown in Fig. 4a, where the femoral neck and the implant are loaded evenly in their upper and lower half. In contrast, in model IIa and model IIb, there is an obvious load shift to the upper and lower edge of the femoral neck, respectively, depending on the DHS location. A similar situation is also shown in model I, where a wedge-shaped groove occurs in the area of the fracture. A goal of performed numerical FE analyses was also to evaluate the DHS stress. The reduced stress σ_{HMH} values are listed in Table 2. The results show that the load at the DHS is considered large enough to achieve and even exceed the value of the yield stress σ_k. The reduced stress on hip plate and cortical screws are indeed close to the yield stress but their values are affected by the TIE contact used to connect the fixing screw with the plate. Maximum values of σ_{HMH} at the plate are in a range of 436.5 MPa (model 0) to 717.3 MPa (model IIb) and those at the lower cortical fixation screw in the range 693.1 MPa (model 0) to 706.6 MPa (model IIa). In contrast, the situation is different at the neck screw, whose tension is not affected by any constraints and the σ_{HMH} is still higher than σ_k. The maximum value of σ_{HMH} has been recorded in a range of 435.3 MPa (model 0) to 716.6 MPa (model I). Model IIa with the reduced stress at the neck screw 713.8 and hip plate 729.8 is associated with the highest risk of the implant failure and re-operation (position 1).

DISCUSSION

Patients treated with the DHS, suffered about a 10% incidence of specific complications in pertrochanteric fractures (Hrubina et al. 2010). Numbers of complications of each type were low, which made statistical evaluation difficult. We focused our consideration on risk positions of the implant (based on the clinical practice) which can lead to osteosynthesis failures. However, there are only a few types of failures ("cut-out", osteosynthetic material breakage...). We thus monitored the situation of each model situation depending on the position of the femoral neck screw based on numerical simulations. We believe that the method of comparing clinical information and model situations will make it possible to demonstrate that expected failures of the osteosynthesis operation procedure (as observed based on the clinical experience) are actually significantly hazardous in term of the origination of specific complications (Rohlmann et al. 1982, Wirtz et al. 1998). In terms of age and sex distribution, our group of patients is similar to these studied by other authors (Kopp et al. 2009, Malkus et al. 2009). There was an obvious association between subsequent complications with need for re-operation and situation of the femoral neck screw in the upper third of the neck (position 1), which led to cutting off the femoral head in 3 of our patients. Clinical monitoring regularly identified the best results in situations where the femoral reduction was done exactly (also in case of opening the fracture line medially, which made possible a controlled fracture compression), with placement of the DHS in the middle of the neck or in the lower third with the subchondral fixation

(positions 2–4). In this subgroup of patients the re-operation rate of 0% to 3% is comparable with other studies (e.g. Barton et al. 2010). The neck screw placement at the head center (not subchondral) involves a 10% risk of re-operation. Nevertheless, in terms of biomechanical consideration, the accurate reduction and operative technique are essential to ensure uneventful fracture healing (Güven et al. 2010, Krischak et al. 2011). These findings are in conformity with results of numerical FE simulations. Our study was limited for a number of reasons. First, the FE analysis always assumes certain simplifications and the bone quality is not taken into account in this analysis. The femoral anatomy of the healthy patient (used for CT scans) could be predictably different from the fracture patients in the study, which is a weakness of the model. However, changes in the femur (geometry, bone mineral density) due to natural ageing are not yet fully understood (Keyak and Falkinstein, Ito et al. 2011). To identify density-elasticity relationships suitable for use in subject-specific FE studies, the development of a benchmark study is also proposed, where the elasticity-density relationship is taken as the variable under study, and a numerical model of the known numerical accuracy predicts experimental strain measurements (Helgason et al. 2008). Secondly, connections were made by the TIE contact, which made any separation of contact surfaces impossible. Another important factor significantly affecting the interpretation of the results obtained, is the nature of the whole investigation. Simulations were modelled as a static task, which is able to describe only a single load moment and system response to this load. In a realistic situation, the DHS and the bone are loaded by repeated pulsed forces (Bergmann et al. 2001, 2004) varying in their amplitude and direction. However, the results of the numerical FE simulations can, in our opinion, offer a number of conclusions and recommendations. All the results obtained show that in terms of biomechanics, the neck screw location is very important during the fracture fixation (Hsueh et al. 2010). The DHS placement directly affects not only the value and type of loading the femur, but also the DHS tension (Couteau et al. 1998). If the neck screw is not in an optimum position, the load can cause excess stress, which may lead to an implant failure. The results in Table 2 show that the femoral neck screw tension exceeded the yield stress σ_k. Values of the reduced stress σ_{HMH} at the end of the neck screw, at the site of the contact with the splint can be considered as parasitic stresses produced due to the contact of the screw with the splint on a very small area (which is a certain type of an imprecision of the finite element method employed). Of course, exceeding the yield stress σ_k in the screw neck was not affected by the coupling method used or by any simplification. The risk of the DHS failure is furthermore considerably enhanced by the cyclic nature of the load to the femoral bone (which was, however, not considered in the analyses performed). The FE analyses performed and their results also show that both fragments of the femur in the area around the screw neck hole, in the plane of the fracture, were susceptible to the permanent degradation of the bone tissue. This condition was caused by significant bending of the screw neck and the consequential pressure on the bone tissue. For long-term DHS survival it is important to have the strain and stress (Birnbaum and Parndorf 2011) equally distributed within the surrounding bone tissue. Any deviation from the optimum position (model 0) considerably affects the stiffness of whole bone-DHS system, thus rapidly increasing the risk of a failure.

The least suitable location of the screw is at the upper third of the femoral neck. The risk of the implant failure was observed from our clinical study in these cases. Our FE model is not able to provide any prediction of complications. This prediction is perhaps impossible due to the nature of the model (one femur, ideal fracture, quality bone tissue), The purpose of our analyses was to support or refute the hypotheses of physicians concerning general trends in introducing the DHS into the bone. Despite the above-mentioned generalizations, it is possible to accept the presented results as representative.

CONCLUSION

The FE numerical simulations performed show the optimum DHS location with minimum implant failure is in the middle of the neck with subchondral fixation. The screw placement in the upper third of the femoral neck is significantly risky. These FE simulations results are reliable as shown by clinical observation. The DHS positioning in the upper third of the neck almost always leads to an implant failure and re-operation and thus we consider this location as a technical mistake.

The authors declare that they have no conflict of interest in this manuscript.

ACKNOWLEDGEMENT

This study was supported by Czech Ministry of Education, Youth and Sports project: “Trans-

disciplinary research in Biomedical Engineering II", No. MSM 6840770012. Its contents are solely the responsibility of the authors and do not necessarily represent the official views of the Czech Ministry of Education, Youth and Sports.

REFERENCES

Baca V, Kachlik D, Horak Z, Stingl, J. The course of osteons in the compact bone of the human proximal femur with clinical and biomechanical significance. Surg Rad Anat. 29: 201–207, 2007.

Baca V, Horak Z, Mikulenka P, Dzupa V. Comparison of an inhomogeneous orthotropic and isotropic material models used for FE analyses. Med Eng Phys. 30: 924–930, 2008.

Barton TM, Gleeson R, Topliss C, Greenwood R, Harries WJ, Chesser TSJ. A comparison of the long gama nail with the sliding hip screw for the treatment of AO/OTA 31-A2 fractures of the proximal part of the femur. J Bone Jt. Surg. 92A: 792–798, 2010.

Bartonicek J, Dousa P, Skala-Rosenbaum J, Kostal R. Trochanteric fractures – current concepts review. Uraz Chir (in Czech). 10: 13–24, 2002.

Baumgaertner MR, Curtin SL, Lindskog DM, Keggi JM. The value of the tip-apex distance in predicting failure of fixation of peritrochanteric fractures of the hip. J Bone Jt Surg. 77A: 1058–1064, 1995.

Bergmann G, Deuretzbacher G, Heller M, Graichen F, Rohlmann A, Strauss J, Duda GN. Hip contact forces and gait patterns from routine activities. J Biomech. 34: 859–871, 2001.

Bergmann G, Graichen F, Rohlmann A. Hip joint contact forces during stumbling. Langebecks Arch Surg. 389: 53–59, 2004.

Birnbaum K, Parndorf T. Finite element model of the proximal femur under consideration of the hip centralizing forces of the iliotibial tract. Clin Biomech. 26: 58–64, 2011.

Bonnaire F, Lein T, Bula P. Trochanteric femoral fractures: Anatomy, biomechanics and choice of implant. Unfallchirurg. 114: 491–500, 2011.

Couteau B, Hobatho MC, Darmana R, Bringola JC, Arlaud JY. Finite element modeling of the vibrational behaviour of the human femur using CT-based individualized geometrical and material properties. J Biomech. 31: 383–386, 1998.

Füchtmeier B, Gebhard F, Lenich A. Complications after pertrochanteric fractures. Unfallchirurg. 114: 479–484, 2011.

Güven M, Yavuz U, Kadioglu B. Importance of screw position in intertrochanteric femoral fractures treated by dynamic hip screw. Orthop Traumatol Surg Res. 96: 21–27, 2010.

Helgason B, Perilli E, Schileo E, Taddei F, Brynjólfsson S, Viceconti M. Mathematical relationships between bone density and mechanical properties: A literature review. Clin Biomech. 23: 135–146, 2008.

Hrubina M, Skotak M, Behounek J. Complications of dynamic hip screw treatment for proximal femoral fractures. Acta Chir Orthop Traum Czech 77: 395–401, 2010.

Hsueh KK, Fang CK, Chen CM, Su YP, Wu HF, Chiu FY. Risk factors in cutout of sliding hip screw in intertrochanteric fractures: an evaluation of 937 patients. Int Orthop. 34: 1273–1276, 2010.

Ito M, Nakata T, Nishida A, Uetani M. Age-related changes in bone density, geometry and biomechanical properties of the proximal femur: CT-based 3D hip structure analysis in normal postmenopausal women. Bone. 48: 627–630, 2011.

Keyak J, Falkinstein Y. Comparison of *in situ* and *in vitro* CT scan-based finite element model predictions of proximal femoral fracture load. Medic Eng Physic. 25: 781–787, 2003.

Kopp L, Edelman K, Obruba P, Prochazka B, Blstaková K, Dzupa V. Mortality risc factors in the elderly with proximal femoral fracture treated surgically. Acta Chir Orthop Traum Czech. 76: 41–46, 2009.

Krischak G, Dürselen L, Röderer G. Treatment of peritrochanteric fractures. Biomechanical considerations. Unfallchirurg. 114: 485–490, 2011.

Malkus T, Vaculik J, Dungl P, Majernicek M. Problems in intertrochanteric fractures. Ortopedie (in Czech). 3: 274–282, 2009.

Rohlmann A, Mössner U, Bergmann G, Kölbel R. Finite-element analysis and experimental investigation of stresses in a femur. J Biomed Eng. 4: 241–246, 1982.

Vaculik J, Malkus T, Majernicek M, Podskubka A, Dungl P. Incidence of proximal femoral fractures. Ortopedie (in Czech). 1: 62–68, 2007.

Viceconti M, Olsen S, Nolte LP, Burton K. Extracting clinically relevant data from finite element situations. Clin Biomech. 20: 451–454, 2005.

Wirtz DC, Pandorf T, Redermacher K. Conception and realization of a physiological justified anisotropic finite-element model of the proximal femur. Z Orthop. 136: A121–A122, 1998.